



HAL
open science

Impact of polyelectrolytes on lysozyme properties in colloidal dispersions

Mbaye Ndour, Jean-Marc Janot, Laurence Soussan, Zaineb Bouaziz, Damien Voiry, Sebastien Balme

► **To cite this version:**

Mbaye Ndour, Jean-Marc Janot, Laurence Soussan, Zaineb Bouaziz, Damien Voiry, et al.. Impact of polyelectrolytes on lysozyme properties in colloidal dispersions. *Colloids and Surfaces B: Biointerfaces*, 2019, 183, pp.110419 -. 10.1016/j.colsurfb.2019.110419 . hal-03488329

HAL Id: hal-03488329

<https://hal.science/hal-03488329v1>

Submitted on 20 Jul 2022

HAL is a multi-disciplinary open access archive for the deposit and dissemination of scientific research documents, whether they are published or not. The documents may come from teaching and research institutions in France or abroad, or from public or private research centers.

L'archive ouverte pluridisciplinaire **HAL**, est destinée au dépôt et à la diffusion de documents scientifiques de niveau recherche, publiés ou non, émanant des établissements d'enseignement et de recherche français ou étrangers, des laboratoires publics ou privés.



Distributed under a Creative Commons Attribution - NonCommercial 4.0 International License

1
2
3
4
5
6
7
8
9
10
11
12
13
14
15
16
17
18
19
20
21
22

Impact of Polyelectrolytes on Lysozyme Properties in Colloidal Dispersions.

Ndaye Ndour, Jean-Marc Janot, Laurence Soussan, Zaineb Bouaziz, Damien Voiry, Sebastien Balme*
Institut Européen des Membranes, IEM – UMR 5635, ENSCM, CNRS, Univ Montpellier, Montpellier, France

Corresponding author: sebastien.balme@umontpellier.fr

Statistical summary: 5198 words; 3 figures, 3 tables

Abstract

In this work, we investigated the impact of different polyelectrolytes (polyacrylic acid, polystyrene sulfonate, dextran sulfate, and chondroitin sulfate) on lysozyme properties when they form colloidal complexes. To this aim, we characterized (i) the size and stability of the different polyelectrolyte-lysozyme complexes upon addition of NaCl (different concentrations) by diffusion light scattering, and (ii) the structure and accessibility of lysozyme active site in such complexes by fluorescence quenching and time resolved fluorescence analysis. We then used these results to explain the antibacterial activity variations among colloidal complexes and compared with free lysozyme. Our findings show that colloidal complexes that are more prone to swelling (i.e., lysozyme complexed with polystyrene sulfonate) are less stable upon salt addition. In these colloids, the enzymatic site is also more accessible. However, the antibacterial activity does not depend on the swelling properties because no large structural modification of the active site occurs.

23 1. Introduction

24 Polyelectrolyte (PE)-protein complexes have been widely studied due to their numerous applications,
25 such as protein delivery, catalysis, biosensing, and protein separation[1]. These complexes adopt
26 different structures (colloidal suspension, gel, and turbid solution[2]) depending on the balance of
27 negative/positive charges. This balance is usually governed by the ratio of protein/PE concentrations
28 and pH[3]. In water media, PE/protein complexes are typically governed by electrostatic interactions,
29 and often become instable at high ionic strength when the salts shield the PE charges[2,4]. In several
30 cases, hydrogen (H-) bonds can compete with electrostatic interactions[1]. Regardless of the nature of
31 the application, a key point of these complexes is the structural modification of the complexed
32 proteins. More specifically for catalysis or biosensing as well as for drug delivery and entrapment, the
33 enzyme active site must be preserved and must remain accessible[5,6] [7,8].

34 Lysozyme is a model of hard protein with a well-known structure[9,10]. It is composed of 129 amino
35 acid residues divided in two main domains: the α -domain made of α -helices, and the β -domain that
36 consists mainly of β -sheets. Between these domains a loop completes the enzymatic site that catalyzes
37 the hydrolysis of the glycosidic β (1-4) linkages between N-acetylglucosamine and N-acetylmuramic
38 acid into peptidoglycans, contributing to lysozyme antibacterial property. From an energetic point of
39 view, lysozyme exhibits a high internal energy of about 60 kJ mol^{-1} due to the large ratio of β -sheets
40 and the four disulfide bonds[10]. As lysozyme is less prone to unfold, it is considered a hard protein.
41 Lysozyme typically maintains its antibacterial properties after adsorption on inorganic material[11] or
42 in the form of amyloid structures obtained after heating at pH 2 for several hours [12]. For this reason,
43 lysozyme is employed for many applications, from medicine to food industry[13]. More recently,
44 lysozyme has been used to solubilize nanoparticles, such as gold[14] and copper[15], opening new
45 avenues for the development of affordable alternatives to gold for sensing[16,17].

46 Lysozyme is often used as a model for basic studies of PE-protein complexes[2]. Such complexes can
47 adopt many different structures (gel, microgel micelle, colloid, precipitate, coacervate) by tuning the
48 lysozyme/PE ratio as well as the PE nature and length[2,18–20]. When mixed with polystyrene

49 sulfonate (PSS) at a [-]/[+] ratio of about 1 ([-] and [+] refer to the concentration of PE and lysozyme,
50 respectively, at neutral pH), such complexes adopt a colloid structure, while lysozyme maintains its
51 antibacterial activity. However, these complexes become unstable in the presence of increasing salt
52 concentrations. With the increase of the [-]/[+] ratio in PSS, lysozyme unfolds and loses its activity[2].
53 To improve the stability of PE-protein complexes in the presence of salts, methoxypoly(ethylene
54 glycol) *-block-poly*(l-aspartic acid sodium salt) has been used to form micelle structures[20].
55 However, encapsulation in the micelle structure modifies the lysozyme α -helix/ β -sheet ratio [20].
56 Consequently, the structure dependence of lysozyme when associated with PE has only been
57 investigated through large structural modifications or antibacterial activity. On the other hand, we
58 recently reported that amyloid fibrillation and/or adsorption of lysozyme on layered material modifies
59 its global structure, whereas the integrity of the active site is less affected[11,12]. Several questions
60 remain unanswered, especially about the correlation between enzymatic activity and the integrity and
61 accessibility of the active site in PE-lysozyme (PE-LYS) complexes.

62 To address these issues, we studied PE-LYS colloids because these complexes are suitable for several
63 applications in catalysis, drug delivery, and entrapment. We considered four different PEs:
64 poly(sodium 4-styrenesulfonate) (PSS), poly(acrylic acid) (PAA), dextran sulfate (DS), and
65 chondroitin 4-sulfate (CS). First, for each PE, we characterized the PE-LYS complex stability in
66 function of the salt concentration by diffusion light scattering. Then, we evaluated the integrity and
67 accessibility of the enzymatic site by fluorescence quenching and time resolved fluorescence analysis.
68 Finally, we analyzed the antibacterial activity of the different PE-LYS complexes.

69 **2. Materiel and methods**

70 ***2.1. Material***

71 Lysozyme ($M=14300 \text{ g mol}^{-1}$, 6297), PSS ($M_w \sim 70000 \text{ g.mol}^{-1}$, 243051), PAA ($M_w \sim 100000 \text{ g.mol}^{-1}$,
72 523925), CS sodium salt from bovine trachea (27042), DS sodium salt from *Leuconostoc spp*
73 ($M_w \sim 6500-10000 \text{ g mol}^{-1}$, D 4911), NaCl (S7653), acrylamide (01700), and hydrazine (225819) were
74 purchased from Sigma-Aldrich. CuSO_4 (22-36/38) was purchased from Prolabo. Non-pathogenic

75 *Staphylococcus epidermidis* (CIP53.124) was purchased from Pasteur Institute Laboratory, Lyon,
76 France. Lysogeny broth (LB) Miller culture medium (ref. n°1214662) was purchased from Fischer
77 Scientific, France.

78 **2.2. Polyelectrolyte-Lysozyme (PE-LYS) colloid complex preparation**

79 PE-LYS complexes were obtained by adding 50 µl of lysozyme solution (concentration = 10 mg ml⁻¹)
80 and 320 µl of PE (PAA, PSS, CS or DS, concentration = 0.5 mg ml⁻¹) to 14.63 ml of deionized water.
81 The resulting colloids were named PAA-LYS, PSS-LYS, CS-LYS, and DS-LYS.

82 **2.3. Antibacterial experiments**

83 Non-pathogenic *Staphylococcus epidermidis* (CIP53.124, from Pasteur Institute Laboratory, Lyon,
84 France) was chosen as surrogate microorganism of bacterial contamination.

85

86 **Preparation of the bacterial suspensions used for antibacterial tests:** For each experiment, a new
87 bacterial suspension was prepared from a frozen *S. epidermidis* aliquot. The frozen inoculum (2 mL)
88 was first transferred in LB medium (10 mL). at 37 °C under constant stirring (110 rpm) for 3h. Then, it
89 was inoculated in fresh LB medium (5% v/v) and incubated at 37 °C under constant stirring (110 rpm)
90 overnight until the bacteria reached the stationary growth phase. Afterwards, bacteria were pelleted by
91 centrifugation (3300 g, 4°C, 20 min) to remove nutrients, and avoid bacterial development in the
92 reactor. The recovered bacterial pellets were suspended in spring water (Cristaline Sainte Cécile,
93 France: [Ca²⁺] = 39 mg L⁻¹, [Mg²⁺] = 25 mg L⁻¹, [Na⁺] = 19 mg L⁻¹, [K⁺] = 1.5 mg L⁻¹, [F⁻] < 0.3 mg L⁻¹,
94 [HCO₃⁻] = 290 mg L⁻¹, [SO₄²⁻] = 5 mg L⁻¹, [Cl⁻] = 4 mg L⁻¹, [NO₃⁻] < 2 mg L⁻¹). The bacterial
95 concentration in the suspensions was determined from the absorbance at 600 nm by using a previously
96 obtained calibration curve. Bacterial cells were finally diluted in spring water to obtain a bacterial
97 suspension in which the cell concentration was about 10⁴ CFU mL⁻¹. Each bacterial suspension was
98 instantly used for the antimicrobial tests.

99 **Counting viable bacteria.** Bacteria were counted using the conventional method of colony counting
100 on agar plates. Each *S. epidermidis* sample was diluted by a factor of 10 in spring water. Each dilution

101 was spread on LB nutrient agar plates, and plates were incubated at 37°C for 24h to allow bacterial
102 colonies to form. Knowing that each colony stemmed from one initial bacterium, the bacterial
103 concentration in each sample was calculated as the mean number of counted colonies divided by the
104 inoculated volume on LB agar plates, by taking into account the corresponding dilution factor. The
105 quantification limit was 10 CFU mL⁻¹. Each counting was done in duplicate and independently.

106 **Assessment of the antibacterial properties of free lysozyme, and PE-LYS colloids:** Bactericidal
107 tests were carried out in a batch mode, in glass Erlenmeyer flasks (25 mL). Reactions were performed
108 in sterile conditions, at 37° C, and under constant stirring (110 rpm) on a rotary shaker. For each test, 9
109 mL of bacterial suspension was mixed with 1 mL of lysozyme solution or PE-LYS colloid suspensions
110 (prepared in deionized water). The final lysozyme concentration was 3 µg L⁻¹ of lysozyme equivalent.
111 The initial bacterial concentration C₀ was precisely determined by the counting method and the mean
112 C₀ was 9.8 ± 0.4 x 10³ CFU mL⁻¹. At the end of the test (3h of incubation at 37° C), the concentration
113 of viable bacteria was measured again using the counting method. Changes in the bacterial
114 concentration were correlated with the bactericidal performances of the tested material. The bacterial
115 concentration decrease was expressed in log-removal values; the log-removal was defined as the
116 logarithm (base 10) ratio of the bacterial concentration C (CFU mL⁻¹) measured at 3h to the initial
117 bacterial concentration C₀ (CFU mL⁻¹). In the case of total removal, a log-removal value of -log (C₀)
118 (i.e., - 4.0) was attributed.

119 ***2.4. Physical characterization***

120 The UV absorbance spectra were recorded on a JASCO V-570 UV-Vis spectrophotometer at 1 nm s⁻¹
121 scanning rate.

122 The diffusion coefficients of PE-LYS colloidal complexes were measured by diffusion light
123 spectroscopy (DLS) (Nanophox, Sympatec, France) at 25°C. From the raw data, the diffusion
124 coefficients were obtained using the Quickfit software[21]. A Levenberg-Marquardt non-linear fit
125 without constraint box was used. Two criteria were considered for the fit quality: 1) the R², and 2) the
126 symmetrical distribution of the residual function. The hydrodynamic radius (*r_H*) of the colloids was

127 deduced from the diffusion coefficient (D) using the Stoke-Einstein equation (equation 1) and
128 assuming a spherical shape:

$$129 \quad D = \frac{k_B T}{6\pi\eta r} \quad (1)$$

130 where k_B , T and η , are the Boltzmann constant, the temperature, and the viscosity, respectively.

131 Time-resolved and steady state fluorescence data were obtained using the time-correlated single-
132 photon counting technique with a previously described home-made set-up[22,23]. Briefly, the
133 excitation wavelength was achieved using a SuperK EXTREME laser (NKT Photonics, model EXR-
134 15) as a continuum pulsed source combined with SuperK EXTEND-UV supercontinuum (NKT
135 Photonics, model DUV). The repetition rate was set to 38.9 MHz; the excitation pulse duration on this
136 device is around 6 ps (full-width-at-half-maximum, FWHM). The fluorescence emission is detected
137 after passing through a polarizer oriented at the magic angle (54.73°) to the polarization of the
138 excitation, through a double monochromator Jobin–Yvon DH10 on a hybrid PMT detector HPM-100-
139 40 (Becker & Hickl). The pulse response function of the equipment was measured by using a diluted
140 suspension of polystyrene nanospheres in water (70 nm of diameter) as scattering solution; FWHM
141 was about 130-160 ps. Decays were collected at a maximum counting rate of 15 kHz in 4096 channels
142 using a SPC-730 acquisition card (Becker & Hickl). All decays were collected with at least $1.5 \cdot 10^6$
143 counts in total. Decay analysis was performed using a Levenberg–Marquardt algorithm. For the
144 analysis, the fluorescence decay law at the magic angle $I_M(t)$ was assumed as the sum of exponentials.
145 Fluorescence lifetime values were calculated from data collected at the magic angle by iterative
146 adjustment after convolution of a pump profile (scattered light) with a sum of exponentials. All details
147 about the calculation of fluorescence lifetime values are given elsewhere[23].

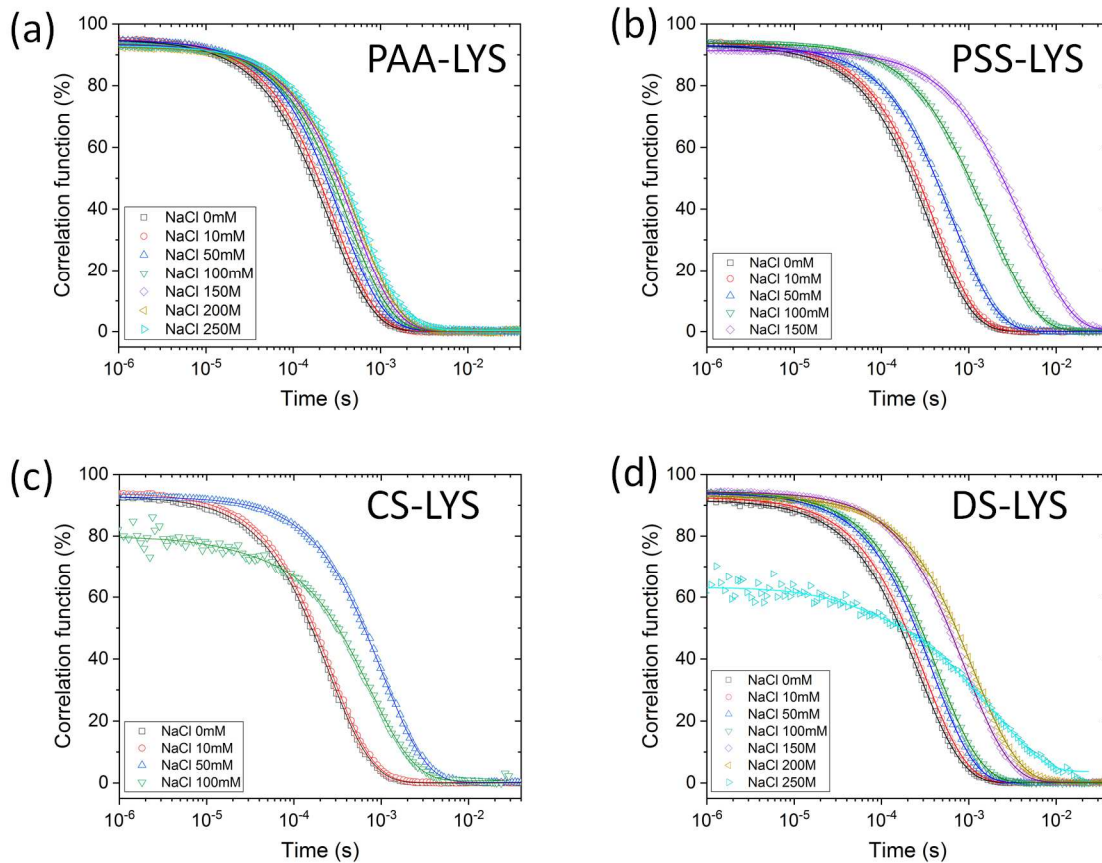
148 **3. Results and discussion**

149 ***3.1. Impact of salinity on PE-LYS colloid stability***

150 PE-LYS complexes were prepared in water using low protein concentration ($33 \mu\text{g ml}^{-1}$). The used [-
151]/[+] ratio was about 0.01 for PSS and PAA, and about 0.2 for CS and DS. Indeed, it was shown that at

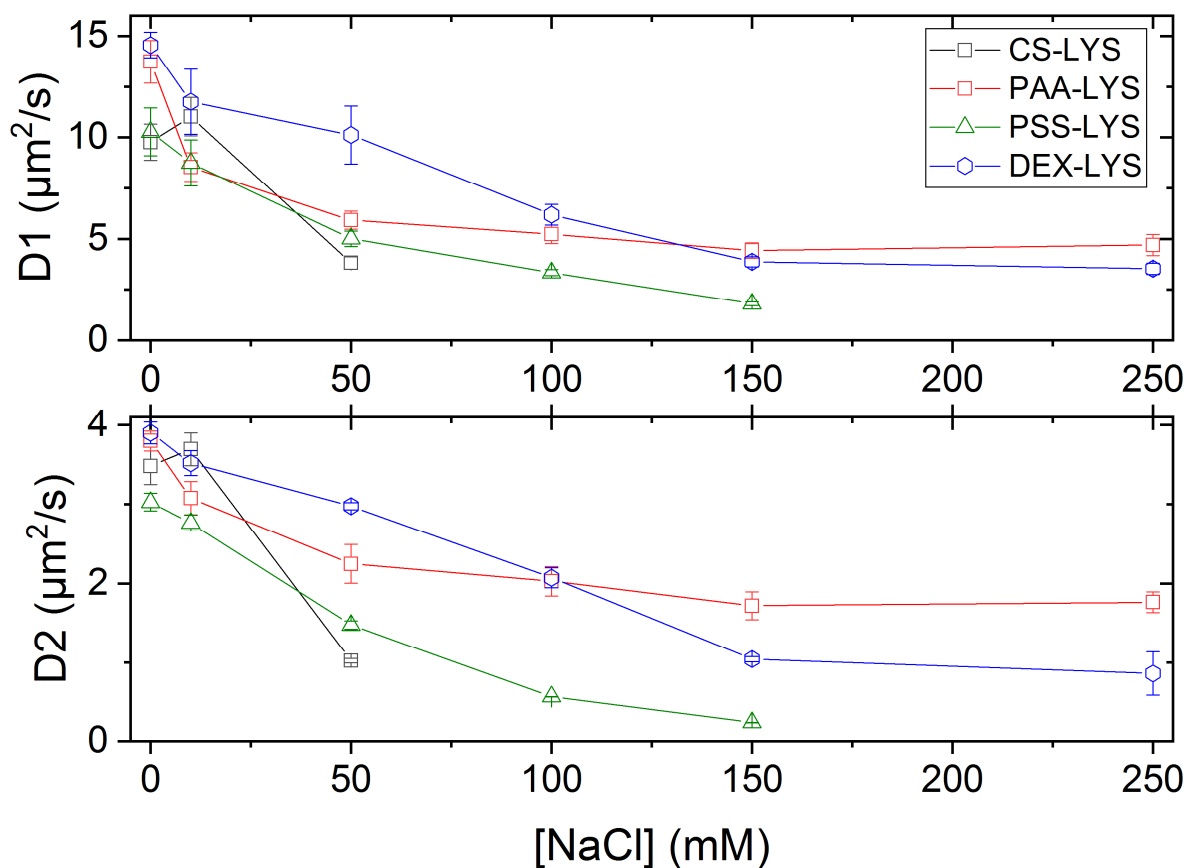
152 [-]/[+] ratios <1, PSS-LYS complexes adopt a colloidal structure[2]. Dynamic light scattering was
153 used to investigate the impact of increasing NaCl concentrations on the diffusion coefficient and
154 stability of PE-LYS colloids (Fig. 1). First, at low NaCl concentrations, the PEs could not be detected
155 by DLS, and lysozyme diffusion coefficient was about $128 \mu\text{m}^2 \text{s}^{-1}$. For the PE-LYS complexes, the fit
156 of the autocorrelation function required two components that depend on the salt concentration (Fig. 2).
157 In water, the fastest component ($D_1 = 13.72 \mu\text{m}^2 \text{s}^{-1}$, $10.27 \mu\text{m}^2 \text{s}^{-1}$, $9.76 \mu\text{m}^2 \text{s}^{-1}$, and $14.55 \mu\text{m}^2 \text{s}^{-1}$ for
158 PAA-LYS, PSS-LYS, CS-LYS, and DS-LYS, respectively) represented the predominant species in the
159 solution (respectively 99.8%, 99.7%, 99.6% and 99.8% according to the pre-exponential factor and
160 assuming a spherical shape for all PE-LYS complexes). It corresponded to spherical colloids with a
161 hydrodynamic radius of 16 nm, 21 nm, 22 nm, and 15 nm for PAA-LYS, PSS-LYS, CS-LYS, and DS-
162 LYS, respectively. Such PE-LYS colloids have been already described[1,3,24]. The slower component
163 ($D_2 = 3.80 \mu\text{m}^2 \text{s}^{-1}$, $3.02 \mu\text{m}^2 \text{s}^{-1}$, $3.48 \mu\text{m}^2 \text{s}^{-1}$, $3.90 \mu\text{m}^2 \text{s}^{-1}$ for PAA-LYS, PSS-LYS, CS-LYS and DS-
164 LYS, respectively) corresponded to larger objects. These large colloids could be assigned to small
165 colloid aggregates that coexist through a dynamic equilibrium. For all PE-LYS colloids, NaCl addition
166 induced a shift of the correlation function toward longer times until signal loss that occurred when the
167 colloids were totally destroyed. For all PE-LYS colloids, the values of the diffusion coefficients D_1
168 and D_2 decreased with the increase of NaCl concentration (Fig. 2). This indicates that the size of the
169 two components of the complexes grew. This observation is not surprising because electrostatic
170 interactions are predominant in the formation of PE-LYS colloids. With the increase of the salt
171 concentration, the PE charges were shielded, inducing two effects. The first one was the swelling of
172 colloids due to the introduction of hydrated ions in the PE-LYS complex. This ultimately led to the
173 colloid dissociation, as indicated experimentally by the loss of the DLS signal. The second effect was
174 the colloid aggregation that was characterized by the decrease of the diffusion coefficient. These two
175 effects co-existed because the aggregation allowed minimizing the colloid global energy,
176 counterbalancing their destabilization due to swelling. Interestingly, the colloid aggregation and
177 stability depended on the PE nature. PAA-LYS complexes were the least affected by NaCl addition,
178 and the colloids were not dissociated in the presence of 300 mM NaCl. On the other hand, PSS-LYS
179 complexes were dissociated in the presence of 200 mM NaCl. Although the electrostatic interactions

180 are the primary factor responsible for colloid formation, weak interactions also can play a role.
181 Typically, PAA carboxylic acid moieties are involved in H-bond formation, whereas PSS is prone to
182 hydrophobic interactions. As lysozyme is a hard protein, it should not be unfolded in the complex.
183 Consequently, its surface should be globally hydrophilic and more prone to H-bond formation than to
184 hydrophobic interactions. H-bonds enter in competition with the screening charge due to the increased
185 salt concentration, thus limiting colloid swelling. In PAA-LYS complexes, the aggregation
186 phenomenon is sufficient to counterbalance the colloid destabilization. Like PAA, DS and CS also can
187 form H-bonds with lysozyme. However, they are less charged than PAA, and this could explain why
188 DS-LYS and CS-LYS colloidal complexes were less stable than PAA-LYS complexes. Moreover,
189 dynamic light scattering experiments showed that upon NaCl addition, DS-LYS colloids were more
190 stable than CS-LYS colloids that were dissociated in the presence of 100 mM NaCl. This result can be
191 explained by the number of anionic moieties on each saccharide unit (2 for DS and 1 for CA).



192

193 Figure 1: Autocorrelation curves obtained by DLS for (a) PAA-LYS complexes, (b) PSS-LYS
 194 complexes, (c) CS-LYS complexes, and (d) DS-LYS complexes at different NaCl concentrations.
 195 Symbols and lines represent the experimental measurements and the fits, respectively.



196

197 Figure 2: Diffusion coefficients measured by DSL as a function of NaCl concentration. D1 is the
 198 shorter and D2 the longer component. Error bars indicate the standard deviation (n=4). In figure
 199 change DEX into DS.

200

201 *3.2. Accessibility and integrity of lysozyme active site*

202 The active site of lysozyme is located between the α - and β -domains of the protein. It contains three
 203 tryptophan residues (Trp62, Trp63, and Trp108) that are important for the enzymatic activity [25].

204 Analysis of its accessibility and integrity showed that at 345 nm, Trp63 fluorescence was quenched by
 205 neighboring disulfide bonds, while 92% of the total fluorescence signal was due to the Trp62 and
 206 Trp108 residues. Their photophysical properties are strongly affected by the environment inside the
 207 active site, and thus by structural modifications [11,12]. Moreover, the fluorescence emission of these
 208 Trp residues is quenched when a molecule, such as acrylamide, enters the active site[26]. Therefore,

209 they represent ideal probes to investigate PE impact on the active site accessibility and integrity and
 210 for correlations with the antibacterial activity.

211 Quantification of the fluorescence decay of free lysozyme (Fig. 3a) showed that in water, the mean
 212 lifetime (τ_0) of lysozyme was 2.34 ns. However, the fluorescence decay fit required four components,
 213 in agreement with our previous work [12]. The shorter one (τ_4 = about 0.01 ns with a yield of 2%)
 214 could be assigned to the contribution of Trp28 and Trp111, two residues located outside the active site
 215 [27]. The three other components (τ_1 = 3.64 ns, τ_2 = 1.62 ns and τ_3 = 0.48 ns with yields of 41 %, 48%
 216 and 9%, respectively) were assigned to Trp62 and Trp108.

217 Table 1: Fluorescence lifetime (τ_i), results (mean \pm standard deviation) for free lysozyme (LYS) and
 218 PE-LYS, obtained with an excitation wavelength of 294 nm and recorded at 345 nm.

	τ_1 (ns)	τ_2 (ns)	τ_3 (ns)	τ_4 (ns)	Y_1 (%)	Y_2 (%)	Y_3 (%)	Y_4 (%)	χ^2	τ_0 (ns)
LYS	3.64 \pm 0. 25	1.62 \pm 0. 12	0.48 \pm 0. 05	0.01 \pm 0. 01	41	48	9	2	1.1 7	2.34 \pm 0.2 6
PAA- LYS	3.86 \pm 0. 22	1.33 \pm 0. 11	0.40 \pm 0. 04	0.01 \pm 0. 01	33	44	20	4	1.1 2	1.93 \pm 0.25
PSS- LYS	4.46 \pm 0. 3	1.62 \pm 0. 13	0.45 \pm 0. 05	0.02 \pm 0. 01	36	45	17	2	1.1 1	2.39 \pm 0.2 8
CS-LYS	4.17 \pm 0. 26	1.58 \pm 0. 11	0.46 \pm 0. 02	0.01 \pm 0. 01	40	44	14	2	1.1 5	2.43 \pm 0.1 9
DS-LYS	4.62 \pm 0. 30	1.70 \pm 0. 10	0.46 \pm 0. 04	0.02 \pm 0. 01	41	42	15	2	1.0 7	2.68 \pm 0.2 2

219
 220 Calculation of the fluorescence decays of lysozyme within PE-LYS complexes also required four
 221 components. The value and yield of the shorter component τ_4 were not significantly modified in the
 222 PE-LYS complexes compared with free lysozyme, suggesting that no large protein structural
 223 modification occurred close to the location of Trp28 and Trp111 inside the protein chain. Conversely,
 224 lysozyme complexation with PE affected differently the value and the yield of the other components.
 225 Indeed, complexation with PAA and DS modified significantly the mean lifetime (τ_0) compared with

226 PSS and CS (Table 1). Conversely, τ_1 and τ_2 values and/or their yields were affected by all PEs. This
 227 could be explained by two hypotheses: (i) PE penetration inside the active site and interaction with
 228 the Trp residues, and/or (ii) modification of the active site structure. These hypotheses were tested
 229 using the acrylamide test. Indeed, if the active site is crowded by PE molecules, acrylamide will not
 230 quench the Trp fluorescence. Addition of acrylamide induced fluorescence quenching in free lysozyme
 231 and also in all PE-LYS colloidal complexes (Fig. 3b). This effect involved both dynamic and static
 232 processes that can be expressed by the following equation:

$$233 \frac{F_0}{F_{\{Q\}}} = (1 + K_{SV}\{Q\})(1 + K_S\{Q\}) \quad (2)$$

234 where F_0 and $F_{\{Q\}}$ are the fluorescence intensity at the quencher concentration =0 and = $\{Q\}$
 235 respectively, K_{SV} is the Stern-Volmer constant (eq. 3) relative to the collisional quenching process[28],
 236 and K_S is the constant of the formation of a ground-state non-fluorescent complex. The Stern-Volmer
 237 constant can be obtained from the linear dependence of $\frac{\tau_0}{\tau_{\{Q\}}}$ as a function of $\{Q\}$ (Fig. 3c). The
 238 K_{SV} Stern-Volmer constant reached 4.65 M^{-1} for free lysozyme and decreased for PE-LYS colloids
 239 (Table 2). A lower K_{SV} could be due to a structural modification or a reduced accessibility of the
 240 active site due to PE presence. To elucidate the origin of K_{SV} reduction, the quenching rate constant
 241 (k_q) was calculated from the fluorescence lifetime value (τ_0) (eq. 3):

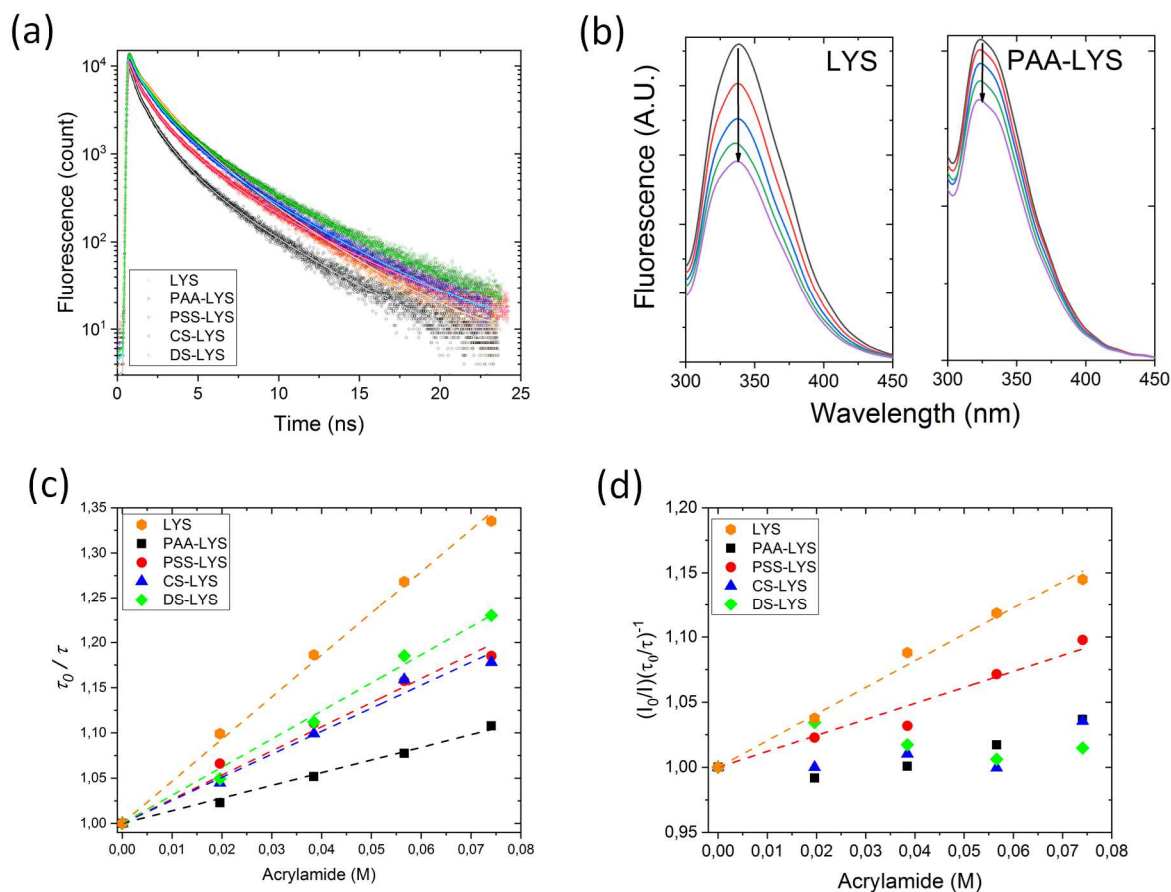
$$242 \frac{\tau_0}{\tau_{\{Q\}}} = 1 + K_{SV}\{Q\} = 1 + k_q\tau_0\{Q\} \quad (3)$$

243 Comparison of the quenching rate constant (k_q) values (Table 2) showed that they were decreased
 244 when lysozyme was complexed with PE. This could directly be interpreted as a decrease of the
 245 acrylamide/Trp collisions. The decrease of dynamic quenching could originate from (i) a modification
 246 of the active structure site, and/or (ii) a decrease of the active site accessibility due to PE steric effect.
 247 As Trp quenching by acrylamide involved also static processes, the K_S was calculated by plotting the
 248 $\frac{I_0}{I} \left(\frac{\tau_0}{\tau_{\{Q\}}} \right)^{-1}$ as a function of acrylamide concentration (Fig. 3d). For free lysozyme in water, a linear
 249 dependence was observed with $K_S = 2.04 \text{ M}^{-1}$. This linear dependence was maintained only when

250 lysozyme was complexed with PSS, but with a lower K_S value (1.22 M^{-1}). This means that the active
 251 site is more accessible in PSS-LYS complexes compared with the PE-LYS made with PAA, CS and
 252 DS.

253

254



255

256 Figure 3: (a) Fluorescence decay (symbol) and fit (line) of free lysozyme (LYS) (orange), PAA-LYS
 257 (black), PSS-LYS (red), CS-LYS (blue) and DS-LYS (green) colloidal complexes. (b) Fluorescence
 258 emission spectra of LYS and PAA-LYS as a function of the acrylamide concentration: 0 mM (black
 259 line), 19 mM (red line), 38 mM (blue line), 56 mM (green line), and 74 mM (violet line). (c) Stern-
 260 Volmer plot (symbol) and linear fit (dash line) for LYS and PE-LYS complexes. (d) Plot of $\frac{I_0}{I} \left(\frac{\tau_0}{\tau} \right)^{-1}$
 261 as a function of acrylamide concentration (symbol), and linear fit (dash line).

262

263 Table 2: Values of the Stern-Volmer K_{SV} constant, quenching constant k_q , and static quenching
 264 constant K_s .

	$K_{SV} [M]^{-1}$	$k_q (10^9)[M \times s]^{-1}$	$K_s [M]^{-1}$
LYS	4.65	2.03	2.04
PAA-LYS	1.40	0.72	N.A.
PSS-LYS	2.67	1.12	1.22
DS- LYS	3.11	1.16	N.A.
CS-LYS	2.55	1.05	N.A.

265

266 In conclusion, our results show that PEs modified the physical properties of the Trp62 and Trp108
 267 residues, and that the active site accessibility was reduced in PE-LYS complexes. The first information
 268 is that the active site was not fully crowded by the PE because acrylamide could still quench Trp
 269 fluorescence. This means that the fluorescence lifetime changes can be assigned to a structural
 270 modification of the active site. This is quite consistent with the fluorescence lifetime results. Indeed, if
 271 PE molecules were present inside the active site, their interaction with the Trp residues should have
 272 modified the fluorescence lifetime values, especially PSS due to the presence of aromatic moieties.
 273 However, our findings indicate that the fluorescence lifetime values were not strongly affected by the
 274 PE, although the photophysical property changes were significant. In addition, it is unlikely that PE
 275 molecules can enter in the active site due to steric hindrance. Thus, the most probable explanation of
 276 the fluorescence lifetime value changes is a structural modification of the active site. Indeed, the active
 277 site is located between the β - and the α -domains of the protein. It is constituted by amino acids
 278 involved in these domains and in the loop that connects them, thus making it prone to local structural
 279 modifications that do not affect the global protein integrity. In some cases, structural modifications of
 280 lysozyme especially in the α -domain do not strongly affect the active site, as previously shown for the

281 lysozyme amyloid structure[12]. This result is consistent with previous reports in which structural
282 modification of lysozyme confined in a PE matrix was highlighted by circular dichroism[20]. The
283 second information is that PEs also play a role in the active site accessibility. Indeed, the acrylamide
284 test results showed that lysozyme active site in PE-LYS complexes formed with PSS is more
285 accessible compared with complexes formed with PAA, CS and DS. This is consistent with the high
286 stability of PAA-LYS colloids upon salt addition (Fig. 1a). Indeed, the interactions (electrostatic and
287 H-bonds) between PAA and LYS are stronger, making the colloid structure more compact.
288 Consequently, acrylamide cannot easily diffuse inside these colloids to form the non-fluorescence
289 complex. Conversely, PSS-LYS colloids swell with the increase of salt concentration, because they are
290 less compact. Therefore, acrylamide can easily diffuse inside the structure. Overall, our results clearly
291 demonstrate that colloids based on CS and DS follow the same trend: the combination of electrostatic
292 interactions and H-bond formation makes these colloids less prone to the formation of acrylamide/Trp
293 complexes.

294 **3.3. Antibacterial activity of PE-LYS colloids**

295 To assess the antibacterial activity of the PE-LYS colloidal complexes against the Gram-positive *S.*
296 *epidermidis*, experiments were performed with the same lysozyme (free or in the colloids)
297 concentration (i.e., 3 $\mu\text{g L}^{-1}$ of lysozyme equivalent). The blank experiment (i.e., bacterial suspension
298 without free lysozyme and PE-LYS) showed that the bacterial concentration remained nearly constant
299 at the end of the 3h incubation (Table 3). As expected, free lysozyme had a strong anti-microbial
300 activity, as indicated by the 2 log-removal value (per absolute value). The PE-LYS colloids exhibited
301 about 1 log-removal values (i.e., 90% of bacteria were killed).. Therefore, our results confirm that
302 lysozyme complexed with PE retains some catalytic activity, and are in agreement with what
303 previously reported for PSS-LYS [2]. It is interesting to note that the PE nature did not influence the
304 log-removal value, indicating that the change in antibacterial activity was not due to a structural
305 modification of the active site, but rather to a decrease of the number of accessible sites, in line with
306 the fluorescence results (section 3.2).

307 Table 3: Bacterial log-removal values (mean \pm standard deviation n=3) obtained after incubation of
308 Gram positive *S. epidermidis* with free lysozyme (LYS) and PE-LYS colloidal complexes for 3 hours.

	Concentration (CFU mL ⁻¹)	Log-removal values (-)
Initial bacterial suspension	$9.8 \pm 0.4 \times 10^3$	
Blank (no LYS and PE-LYS) at 3h	$8.5 \pm 0.4 \times 10^3$	- 0.1
LYS at 3h	$4.0 \pm 0.4 \times 10^1$	- 2.4
PAA-LYS at 3h	$1.1 \pm 0.1 \times 10^3$	- 0.9
PSS-LYS at 3h	$1.2 \pm 0.2 \times 10^3$	- 0.9
DS-LYS at 3h	$9.6 \pm 0.3 \times 10^2$	- 1.0
CS-LYS at 3h	$1.2 \pm 0.1 \times 10^3$	- 0.9

309

310

311 4. Conclusion

312 We investigated the properties of lysozyme involved in colloids with different polyanions. Our results
313 highlight that the PE nature strongly influences the size and stability of PE-LYS colloidal complexes
314 as well as the antibacterial properties of lysozyme when complexed with PEs. Colloids made with
315 PAA, where both electrostatic interactions and H-bond formation are involved, were more compact
316 and more stable than those obtained with PSS. However, the enzyme active sites were less accessible
317 to acrylamide. The complexes formed with polysaccharides (DS and CS) also involved electrostatic
318 interactions and H-bond formation. This led to a compact complex structure that did not allow the
319 formation of Trp-acrylamide complexes. However, due to their lower charge density, compared with
320 DS (and PAA), CS are less stable upon salt addition. On the basis of the fluorescence results, the
321 decreased antibacterial activity observed when lysozyme was complexed with PEs can be explained by
322 the reduced accessibility and a structural modification of the enzyme active site. Our results highlight
323 the role of the PE-LYS structure as a key factor for understanding lysozyme activity.

324

325 Acknowledgements

326 The authors would like to acknowledge the “Institut Européen des Membranes (IEM)-UMR 5635” for
327 supporting this study through the health project PS1-2017.

328 **References**

- 329 [1] C.L. Cooper, P.L. Dubin, A.B. Kayitmazer, S. Turksen, Polyelectrolyte-protein complexes,
330 *Curr. Opin. Colloid Interface Sci.* 10 (2005) 52–78. doi:10.1016/j.cocis.2005.05.007.
- 331 [2] F. Cousin, J. Gummel, S. Combet, F. Boué, The model Lysozyme-PSSNa system for
332 electrostatic complexation: Similarities and differences with complex coacervation, *Adv.*
333 *Colloid Interface Sci.* 167 (2011) 71–84. doi:10.1016/j.cis.2011.05.007.
- 334 [3] J.M. Park, B.B. Muhoberac, P.L. Dubin, J. Xia, Effects of Protein Charge Heterogeneity in
335 Protein-Polyelectrolyte Complexation, *Macromolecules.* 25 (1992) 290–295.
336 doi:10.1021/ma00027a047.
- 337 [4] J. Gummel, F. Cousin, F. Boué, Counterions release from electrostatic complexes of
338 polyelectrolytes and proteins of opposite charge: A direct measurement, *J. Am. Chem. Soc.* 129
339 (2007) 5806–5807. doi:10.1021/ja070414t.
- 340 [5] B. Krajewska, Application of chitin- and chitosan-based materials for enzyme immobilizations:
341 A review, *Enzyme Microb. Technol.* 35 (2004) 126–139. doi:10.1016/j.enzmictec.2003.12.013.
- 342 [6] F. Caruso, C. Schüler, Enzyme multilayers on colloid particles: Assembly, stability, and
343 enzymatic activity, *Langmuir.* 16 (2000) 9595–9603. doi:10.1021/la000942h.
- 344 [7] L.E. Bromberg, E.S. Ron, Temperature-responsive gels and thermogelling polymer matrixes
345 for protein and peptide delivery, *Adv. Drug Deliv. Rev.* 31 (1998) 197–221.
- 346 [8] N.A. Peppas, W. Leobandung, Stimuli-sensitive hydrogels: Ideal carriers for chronobiology
347 and chronotherapy, *J. Biomater. Sci. Polym. Ed.* 15 (2004) 125–144.
348 doi:10.1163/156856204322793539.
- 349 [9] T. Arai, W. Norde, The behavior of some model proteins at solid-liquid interfaces 1.

- 350 Adsorption from single protein solutions, *Colloids and Surfaces*. 51 (1990) 1–15.
351 doi:10.1016/0166-6622(90)80127-P.
- 352 [10] J. Koo, M. Erkkamp, S. Grobelny, R. Steitz, C. Czeslik, Pressure-induced protein adsorption at
353 aqueous-solid interfaces, *Langmuir*. 29 (2013) 8025–8030. doi:10.1021/la401296f.
- 354 [11] S. Balme, R. Guégan, J.-M. Janot, M. Jaber, M. Lepoitevin, P. Dejardin, X. Bourrat, M.
355 Motelica-Heino, Structure, orientation and stability of lysozyme confined in layered materials,
356 *Soft Matter*. 9 (2013). doi:10.1039/c3sm27880h.
- 357 [12] Z. Bouaziz, L. Soussan, J.-M. Janot, M. Lepoitevin, M. Bechelany, M.A. Djebbi, A.B.H.
358 Amara, S. Balme, Structure and antibacterial activity relationships of native and amyloid fibril
359 lysozyme loaded on layered double hydroxide, *Colloids Surfaces B Biointerfaces*. 157 (2017).
360 doi:10.1016/j.colsurfb.2017.05.050.
- 361 [13] T. Wu, Q. Jiang, D. Wuc, Y. Hu, S. Chen, T. Ding, X. Ye, D. Liu, J. Chen, What is new in
362 lysozyme research and its application in food industry? -A review, *Food Chem.* (2018).
363 doi:10.1016/j.foodchem.2018.09.017.
- 364 [14] H. Wei, Z. Wang, J. Zhang, S. House, Y.G. Gao, L. Yang, H. Robinson, L.H. Tan, H. Xing, C.
365 Hou, I.M. Robertson, J.M. Zuo, Y. Lu, Time-dependent, protein-directed growth of gold
366 nanoparticles within a single crystal of lysozyme, *Nat. Nanotechnol.* 6 (2011) 93–97.
367 doi:10.1038/nnano.2010.280.
- 368 [15] R. Ghosh, A.K. Sahoo, S.S. Ghosh, A. Paul, A. Chattopadhyay, Blue-emitting copper
369 nanoclusters synthesized in the presence of lysozyme as candidates for cell labeling, *ACS*
370 *Appl. Mater. Interfaces*. 6 (2014) 3822–3828. doi:10.1021/am500040t.
- 371 [16] X. Hu, T. Liu, Y. Zhuang, W. Wang, Y. Li, W. Fan, Y. Huang, Recent advances in the
372 analytical applications of copper nanoclusters, *TrAC - Trends Anal. Chem.* 77 (2016) 66–75.
373 doi:10.1016/j.trac.2015.12.013.
- 374 [17] Y. Guo, F. Cao, X. Lei, L. Mang, S. Cheng, J. Song, Fluorescent copper nanoparticles: Recent

- 375 advances in synthesis and applications for sensing metal ions, *Nanoscale*. 8 (2016) 4852–4863.
376 doi:10.1039/c6nr00145a.
- 377 [18] C. Johansson, P. Hansson, M. Malmsten, Interaction between lysozyme and poly(acrylic acid)
378 microgels, *J. Colloid Interface Sci.* 316 (2007) 350–359. doi:10.1016/j.jcis.2007.07.052.
- 379 [19] C. Johansson, J. Gernandt, M. Bradley, B. Vincent, P. Hansson, Interaction between lysozyme
380 and colloidal poly(NIPAM-co-acrylic acid) microgels, *J. Colloid Interface Sci.* 347 (2010)
381 241–251. doi:10.1016/j.jcis.2010.03.072.
- 382 [20] F.G. Wu, Y.W. Jiang, Z. Chen, Z.W. Yu, Folding Behaviors of Protein (Lysozyme) Confined
383 in Polyelectrolyte Complex Micelle, *Langmuir*. 32 (2016) 3655–3664.
384 doi:10.1021/acs.langmuir.6b00235.
- 385 [21] J. Krieger, J. Langowski, QuickFit 3.0 : A data evaluation application for biophysics, (2015).
386 <http://www.dkfz.de/Macromol/quickfit/>.
- 387 [22] V. Tangaraj, J.-M. Janot, M. Jaber, M. Bechelany, S. Balme, Adsorption and photophysical
388 properties of fluorescent dyes over montmorillonite and saponite modified by surfactant,
389 *Chemosphere*. 184 (2017). doi:10.1016/j.chemosphere.2017.06.126.
- 390 [23] S. Balme, J.-M. Janot, P. Déjardin, P. Seta, Highly efficient fluorescent label unquenched by
391 protein interaction to probe the avidin rotational motion, *J. Photochem. Photobiol. A Chem.*
392 184 (2006). doi:10.1016/j.jphotochem.2006.04.016.
- 393 [24] F. Cousin, J. Gummel, D. Ung, F. Boué, Polyelectrolyte-protein complexes: Structure and
394 conformation of each specie revealed by SANS, *Langmuir*. 21 (2005) 9675–9688.
395 doi:10.1021/la0510174.
- 396 [25] E. Nishimoto, S. Yamashita, A.G. Szabo, T. Imoto, Internal motion of lysozyme studied by
397 time-resolved fluorescence depolarization of tryptophan residues, *Biochemistry*. 37 (1998)
398 5599–5607. doi:10.1021/bi9718651.

- 399 [26] Y. Tokunaga, Y. Sakakibara, Y. Kamada, K.I. Watanabe, Y. Sugimoto, Analysis of core region
400 from egg white lysozyme forming amyloid fibrils, *Int. J. Biol. Sci.* 9 (2013) 219.
401 doi:10.7150/ijbs.5380.
- 402 [27] S. Yamashita, E. Nishimoto, N. Yamasaki, The Steady State and Time-resolved Fluorescence
403 Studies on the Lysozyme-Ligand Interaction, *Biosci. Biotechnol. Biochem.* 59 (2009) 1255–
404 1261. doi:10.1271/bbb.59.1255.
- 405 [28] A.M. Edwards M., E. Silva S., Exposure of tryptophanyl residues in α -lactalbumin and
406 lysozyme - Quantitative determination by fluorescence quenching studies, *Radiat. Environ.*
407 *Biophys.* 25 (1986) 113–122. doi:10.1007/BF01211735.
- 408 [

Polyelectrolytes



Lysozyme

